Universal Journal of Physics and Application 2(1): 10-13, 2014 http://www.hrpub.org
DOI: 10.13189/ujpa.2014.020103

Synthesis, Crystallographic and Magnetic Properties of Mn Doped ZnO Nanocrystals Via Solid State Reaction Technique

V. D. Mote[1],B. N. Dole[2,*]

[1]Department of Physics, Dayanand Science College, Latur-413512, India
[2]Advance Materials Research Lab., Dept. of Physics, Dr. B. A. Marathwada, University, Aurangabad - 431 004, India
*Corresponding Author: drbndole@yahoo.com

Abstract The polycrystalline undoped and Mn doped ZnO ($Zn_{0.85}Mn_{0.15}O$) nanocrystals were successfully synthesized using solid state reaction technique. The X-ray diffraction (XRD) studies of pure ZnO and Mn doped ZnO nanocrystals exhibit the wurtzite structure (hexagonal phase, space group $P6_3mc$) with high crystallinity and also without any impurity phases. Surface morphology and particle size were carried out using transmission electron microscopy (TEM). It shows that these nanoparticles are of hexagonal phase ZnO mostly in spherical shape with average diameter of the nanocrystals were in the range 30 -100 nm. The magnetic measurements by vibrating sample magnetometer (VSM) clearly indicate that the pure ZnO nanocrystals are in ferromagnetic nature and Mn doped ZnO nanocrystals exhibit co-existence of paramagnetic and ferromagnetic behavior at room temperature.

Keywords DMS, ZnO, Nanocrystals, Magnetization

1. Introduction

Zinc oxide (ZnO) is an excellent electronic and photonic material having a wide bandgap ($E_g \approx 3.27$ eV), a large exciton binding energy of 60 meV, high chemical stability, good piezoelectric properties, nontoxicity, and biocompatibility. The novel properties of nanoscale zinc oxide particles have found applications in a variety of applications such as luminescence [1–3], varistors [4, 5], solar cells [6], gas sensors [7, 8], etc.. Previously, ZnO nanoparticles have been prepared by techniques such as the sol–gel method [7–9], precipitation [10, 11], thermal decomposition [12, 13], hydrothermal synthesis [14, 15], and spray pyrolysis [16]. However, all of these approaches use calcination or sintering. Moreover, most of them need complex apparatus, or processing, and in many cases they involve toxic reagents or additives. The relatively high temperature, complexity and toxicity of these techniques restrict their wide spread application.

Therefore, the efforts of seeking nontoxic, simple, low-cost and high-yield synthetic methods for preparing nanometer materials are being keenly pursued.

The origin of ferromagnetic behavior in Mn-doped ZnO is far from being understood with some research groups have claimed that ferromagnetism in TM-doped ZnO is external and comes from impurities [17], while other groups have reported that ferromagnetism in the same TM-doped ZnO prepared using the same preparation method is intrinsic to the ZnO:TM matrix [18]. However, in addition to the transition metal doping effect, structural defects such as oxygen vacancies were proposed to influence the ferromagnetic state of the oxide Diluted Magnetic Semiconductors (DMS) [19]. Recently, a number of experiments shown the correlation between the ferromagnetic behavior and the concentration of structural defects, either Zn interstitials [20] or oxygen vacancies [21] incorporated into the ZnO host lattice giving evidence that ferromagnetism in ZnO: Mn is mediated by donor-bound carrier

Grinding processing has been routinely used as a scalable physical technique to directly break bulk materials to form fine particles upto nanoscale. In the present study, we use conventional solid state reaction technique for synthesis of $Zn_{1-x}Mn_xO$ nanoparticles owing to its simplicity, low cost, easy handling and low temperature with controlled average grain size. The structural and magnetic properties were investigated using X-ray diffraction (XRD), Transmission electron microscopic (TEM) and Vibrating sample magnetometer (VSM).Such results are reported in this paper qualitatively and quantitatively.

2. Experimental Details

The samples $Zn_{1-x}Mn_xO$ with composition (x= 0.00 and 0.15) were synthesized by conventional solid state route.

Appropriate amount of ZnO and MnO_2 were mixed and ground in an agate mortar by pestle. The resulting powder was calcined at 450^0C for 8h in air and thereafter it was furnace cooled. The resulting materials were reground and again calcined as above. After calcinations the mixture was ground and pelletized using automatic KBr press technosearch instruments. Finally, these pellets were sintered at 450^0 C in air for 8h each followed by furnace cooling up to room temperature. The crystal structure of the sample synthesized in the present work was studied by using X-ray diffractometer (Model: PW-3710) employing Cuk_α (λ = 1.5406A^o) radiation. To study the sample morphology, the powders were ultrasonically mixed with ethanol and suspended on a Cu mesh, which was the sample holder of a transmission electron microscope (TEM) operated at 200 kV. The magnetic properties of the $Zn_{1-x}Mn_xO$ samples were investigated by vibrating sample magnetometer (VSM) (LAKE SHORE 7307 Model) at room temperature.

3. Results and Discussion

3.1 Structural Properties

Figures 1(a) and (b) respectively show the XRD pattern of the typical undoped ZnO and Mn doped ZnO nanocrystals. In the diffraction pattern, all the observed diffraction peaks of both samples can be indexed to the hexagonal wurtzite structure of ZnO (JCPDS card No 36-1451). All peak positions and relative peak intensities of the ZnO nanocrystals agree well with those of the standard XRD pattern and no characteristic peaks of impurities are observed, indicating that the ZnO nanocrystals is of high purity. The phase structure of ZnO nanocrystals belong to a wurtzite structure (hexagonal phase, space group *P*63*mc*). Moreover, all diffraction peaks of the sample show stronger peak intensities, indicating that the obtained ZnO nanocrystals have high crystallinity. However, the cell volume of the wurtzite phase of ZnO:Mn samples was found to shrink from 47.69 $(A^0)^3$ and 47.56 $(A^0)^3$ for pure ZnO, possibly due to the decrease of defects which consistent with the crystals improvement for Mn doped as revealed from XRD spectrum as shown Fig. 1.The mean crystallite size of a powder sample was calculated from the full width at half-maximum (FWHM) of the diffraction peak according to the Scherrer equation (i.e. $D = 0.9\lambda/\beta\cdot\cos\theta$), where λ- is the wave length of the X- ray diffraction, θ- is the diffraction angle and β- is full width at half maximum (FWHM). The average crystalline size of pure ZnO and $Zn_{0.85}Mn_{0.15}O$ nanocrystals were estimated to be about 36 nm and 34 nm respectively after appropriate background correction from X-ray line broadening the lattice parameters evaluated from XRD data of $Zn_{0.85}Mn_{0.15}O$ are a = 3.2507 A^0 and c = 5.2112 A^0, which are closer to the ZnO (a = 3.2480 ± 0.002 A^0, c = 5.2064 ± 0.003 A^0) revealing that the doping of Mn does not affect the wurtzite structure of zinc oxide.

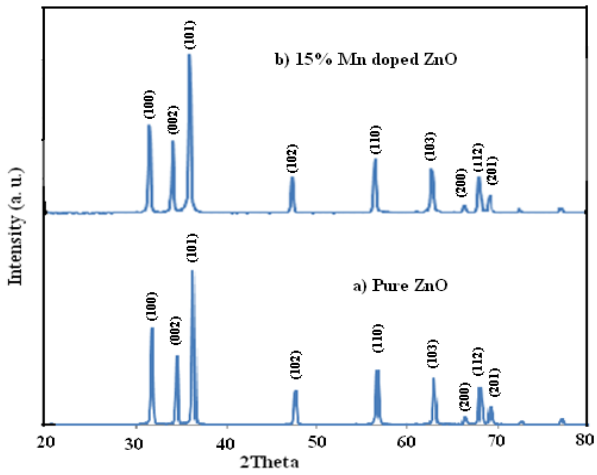

Figure 1. XRD pattern for a) pure ZnO and b) Mn doped ZnO ($Zn_{0.85}Mn_{0.15}O$) samples

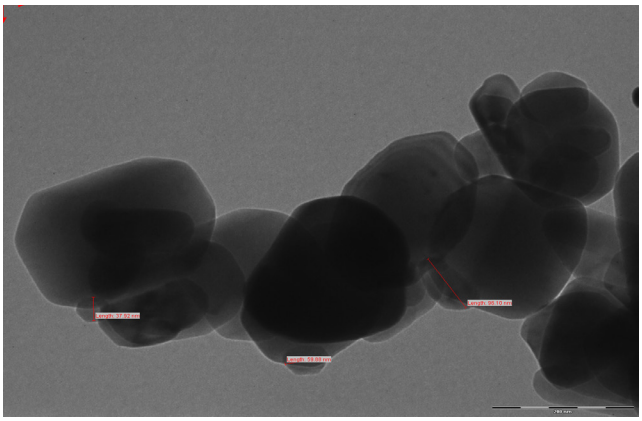

Figure 2. (a). TEM images of ZnO nanocrystals.

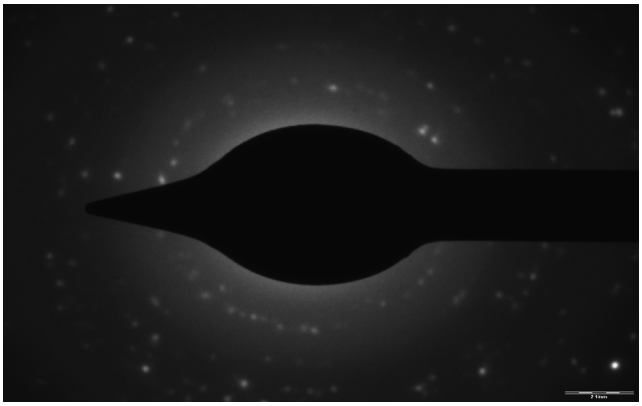

Figure 2. (b). SAED pattern of ZnO nanocrystals.

The particle size and morphology of a sample was characterized by transmission electron microscopy. The typical bright field TEM images for pure sample are shown in figure 2(a). The TEM study of ZnO nanocrystals indicates that most of the nanoparticles are nearly spherical and hexagonal shape. From the micrograph their average grain sizes observed in the range of 30 -100 nm and the mean grain size is 35 nm, the selected-area electron diffraction (SAED) pattern as shown in figure 2(a), taken from the TEM image as

shown in figure 2(a). It can be indexed to the reflection of wurtzite ZnO structure and shows diffraction intensity associated with crystalline ZnO, which is consistent with the XRD results. These nanoparticles have clear borders, illustrating that they are well crystallized.

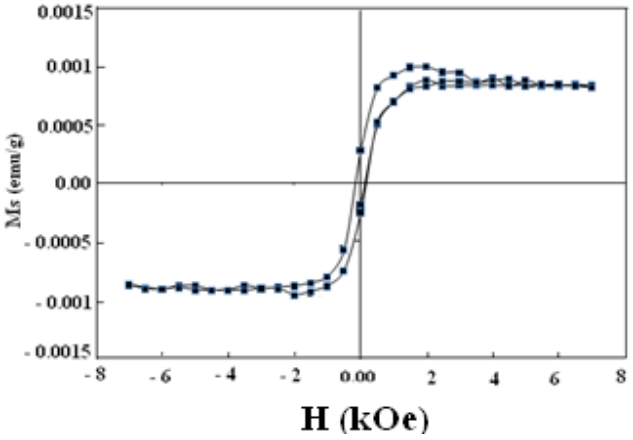

Figure 3. (a). Magnetization vs. Field curve for ZnO at room temperature

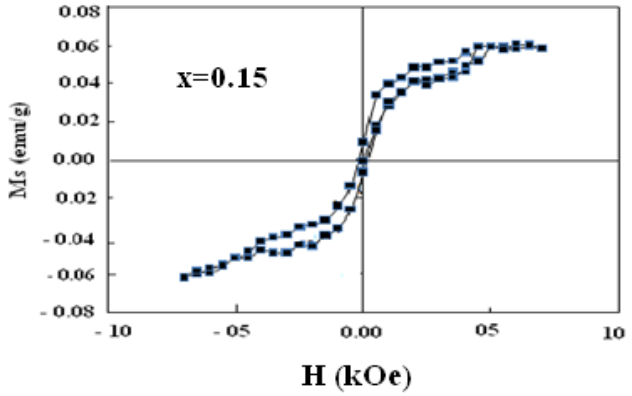

Figure 3. (b). Magnetization vs. Field curve for $Zn_{0.85}Mn_{0.15}O$ at room temperature

3.2. Magnetic Properties

Figures 3(a) and 3(b) show the magnetic hysteresis M-H curves (field dependence of magnetization) for the pure ZnO and Mn substituted ZnO ($Zn_{0.85}Mn_{0.15}O$) nanocrystals measured at room temperature. It is clear that pure ZnO exhibit ferromagnetic behavior and Mn doped ZnO sample shows paramagnetism and ferromagnetism behaviour. Further, it is evident from figures that the saturation magnetization (Ms) increases as Mn doping. The saturation magnetization (Ms) values obtained from hysteresis loops are 9.97×10^{-4} emu/g for pure ZnO and 6.09×10^{-4} emu/g for Mn doped ZnO nanocrystals samples. The values of coercivity (H_c) both samples are 280 G for pure ZnO and 178 G for Mn doped ZnO nanocrystals. The ZnMnO nanocrystals can also show FM properties by carefully control over doping speciation and concentration. Several assumptions have been addressed at up till now: the role of the secondary phase, the connection between defects and magnetism, oxygen vacancy, etc [22-24]. In order to understand the magnetic behavior of the samples, it is not clear whether the ferromagnetism originates from secondary phase formation, because (a) metallic Mn is antiferromagnetic and (b) nearly all of the possible Mn-based binary and ternary oxide candidates are antiferromagnetic except Mn_3O_4 which is ferromagnetic with a curie temperature of only 46 K in thin film [25]. Further, Our results show that the pure ZnO nanocrystals have ferromagnetism due to the alternation of the semiconductor electronic configuration can be present in the absence of magnetic ions [26] and also Mn doped ZnO nanocrystals clearly indicate the coexistence of para and ferromagnetic nature. These results are consistent with the more recent study [27], in which ferromagnetism is mediated by shallow donor electrons that form bound magnetic polarons, which overlap to create a spin split impurity band. In ZnO, slowly Mn doping usually results in n- type ZnO. It is found that when Mn concentration enhances in ZnO nanocrystals upto 15% there is coexistence of para and ferromagnetism but in reported literature system shows paramagnetism [27]. On the other hand, intrinsic defects, oxygen vacancy, unreacted MnO_2 [28], such as act as shallow donors in ZnO [10]. Then, according to Coey et al. [19], the room temperature ferromagnetism in $Zn_{1-x}Mn_xO$ (x = 0.15) nanocrystals would originates from the long range Mn^{2+}-Mn^{2+} ferromagnetic coupling mediated by shallow donor electron.

4. Conclusion

Nanocrystals of $Zn_{1-x}Mn_xO$ (x= 0.00 and 0.15) have been successfully prepared using solid state reaction technique. Microstructure analysis confirms the single phase hexagonal wurtzite structure for pure ZnO and Mn doped ZnO nanocrystals respectively. The particle size and morphology of the $Zn_{1-x}Mn_xO$ nanocrystals have been determined by transmission electron microscopy. It indicates that the particles size lies in the range 30 - 100 nm, which is consistent with the result obtained from the XRD data. The selected-area electron diffraction (SAED) pattern shows that the nanocrystals are in crystalline nature. Magnetic hysteresis curves show that the co-existence of paramagnetic and ferromagnetic behavior in Mn doped ZnO nanocrystals but in pure ZnO nanocrystals show only ferromagnetic phase exist even at room temperature may due to alteration of semiconductor electronic configuration.

REFERENCES

[1] A. van Dijken, E. A. Meulenkamp, D. Vanmaekelbergh, A. Meijerink, J. Luminesc. 87–89, 454 (2000).

[2] L. Guo, S. H. Yang, C .L. Yang, P. Yu, J. N. Wang, W. K. Ge,

G. K. L. Wong, Chem. Mater. 12, 2268 (2000).

[3] Y. Feng, Y. X. Zhou, Y. Q. Liu, G. B. Zhang, X. Y. Zhang, J. Luminesc. 119/120, 233 (2006).

[4] S. Hingorani, V. Pillai, P. Kumar, M. S. Multani, D. O. Shah, Mater. Res. Bull. 28, 1303.(1993).

[5] S. C. Pillai, J. M. Kelly, D. E. McCormack, P. O'Brien, R. Ramesh, J. Mater. Chem. 13, 2586 (2003).

[6] W. J. E. Beek, M. M. Wienk, R. A. J. Janssen, Adv. Mater. 16, 1009 (2004).

[7] M. Epifani, R. Diaz, J. Arbiol, E. Comini, N. Sergent, T. Pagnier, P. Siciliano, G. Taglia, J. R. Morante, Adv. Funct. Mater. 16, 1488 (2006).

[8] H. X. Tang, M. Yan, X. F. Ma, H. Zhang, M. Wang, D. R. Yang, Sens. Actuators B 113, 324 (2006).

[9] J. H. Lee, K. H. Ko, B.O. Park, J. Cryst. Growth 247, 119 (2003).

[10] L. N.Wang, M. Muhammed, J. Mater. Chem. 9, 2871 (1999).

[11] J. E. Rodr´ıguez-Pa´ez, A. C. Caballero, M. Villegas, C. Moure, P. Dur´an, J. F. Fern´andez, J. Eur. Ceram. Soc. 21, 925 (2001).

[12] Y. Yang, H. L. Chen, B. Zhao, X. M. Bao, J. Cryst. Growth 263, 447 (2004).

[13] P. D. Cozzoli, M. L. Curri, A. Agostiano, G. Leo, M. Lomascolo, J. Phys. Chem. B 107, 4756 (2003).

[14] H. Y. Xu, H. Wang, Y. C. Zhang, W. L. He, M. K. Zhu, B. Wang, H. Yan, Ceram. Int. 30, 93 (2004).

[15] K. Sue, K. Kimura, K. Arai, Mater. Lett. 58, 3229 (2004).

[16] T. Tani, L. Madler, S.E. Pratsinis, J. Nanopart. Res. 4, 337 (2002)

[17] Y. M. Kim, M. Yoon, I. -W. Park, Y. J. Park, and J. H. Lyou, Solid State Commun. 129, 175 (2004).

[18] L. Q. Liu, B. Xiang, X. Z. Zhang, Y. Zhang, and D. P. Yu, Appl. Phys. Lett. 88, 63104 (2006).

[19] J. M. D. Coey, M. Venkatesan, and C. B. Fitzgerald, Nat. Mater. 4, 173 (2005).

[20] K. R. Kittilstved, W. K. Liu, and D. R. Gamelin, Nat. Mater. 5, 291 (2006).

[21] N. H. Hong, J. Sakai, N. T. Huong, N. Poirot, and A. Ruyter, Phys. Rev. B 72, 45336 (2005).

[22] S. J. Pearton, D. P. Norton, and K. Ip. Progress in Mater. Sci. 50, 293 (2005)

[23] M. Venkatesan, C. B. Fitzgerald, and J. M. D. Coey, Nature 430, 630 (2004)

[24] O. Eriksson, L. Bergqvist, and B. J. Sanyal, Phys. Condens. Matter. 16, S5481.

[25] A. Chartier, P. D. Arco, and R. Dovesi, Phys. Rev. B 60, 14042 (1999).

[26] M. A. Garcia J. M. Merino, E. Fernandez Pinel, A. Quesada, J. de la Venta, M. L. Ruiz Gonzalez, G. R. Castro, P. Crespo, J. Liopis, J. M. Gonzalez-Calbet, and A. Hernando, Nano letters 7, 1489 (2007).

[27] H. Gui-jun, W. Jin.bin, Z. Xiang-li, Z. Gong-cheng, and Y. Hal-long, Optoelectronics Letts. 2, 6 (2006).

[28] J. L. Costa-Kramer, F. Briones, J. F. Fernandez, A. C. Caballero, M. Villegas, M. Daz, M. A. Garcia and A. Hernando, Nanotechnology 16, 214-218 (2005).